

# Accepted Manuscript

The origin of cycling enhanced capacity of Ni/NiO species confined on nitrogen doped carbon nanotubes for lithium-ion battery anodes

Yidong Luo, Mouyi Weng, Jiaxin Zheng, Qinghua Zhang, Bingqing Xu, Shaoqing Song, Yang Shen, Yuanhua Lin, Feng Pan, Cewen Nan



PII: S0925-8388(18)31140-X

DOI: [10.1016/j.jallcom.2018.03.269](https://doi.org/10.1016/j.jallcom.2018.03.269)

Reference: JALCOM 45499

To appear in: *Journal of Alloys and Compounds*

Received Date: 30 November 2017

Revised Date: 7 March 2018

Accepted Date: 21 March 2018

Please cite this article as: Y. Luo, M. Weng, J. Zheng, Q. Zhang, B. Xu, S. Song, Y. Shen, Y. Lin, F. Pan, C. Nan, The origin of cycling enhanced capacity of Ni/NiO species confined on nitrogen doped carbon nanotubes for lithium-ion battery anodes, *Journal of Alloys and Compounds* (2018), doi: 10.1016/j.jallcom.2018.03.269.

This is a PDF file of an unedited manuscript that has been accepted for publication. As a service to our customers we are providing this early version of the manuscript. The manuscript will undergo copyediting, typesetting, and review of the resulting proof before it is published in its final form. Please note that during the production process errors may be discovered which could affect the content, and all legal disclaimers that apply to the journal pertain.

# The origin of cycling enhanced capacity of Ni/NiO species confined on nitrogen doped carbon nanotubes for lithium-ion battery anodes

Yidong Luo<sup>a, #</sup>, Mouyi Weng<sup>b, #</sup>, Jiabin Zheng<sup>b</sup>, Qinghua Zhang<sup>a</sup>, Bingqing Xu<sup>a</sup>, Shaoqing Song<sup>c</sup>, Yang Shen<sup>a</sup>, Yuanhua Lin<sup>a, \*</sup>, Feng Pan<sup>b, \*</sup>, and Cewen Nan<sup>a</sup>

<sup>a</sup>State Key Laboratory of New Ceramics and Fine Processing, School of Materials Science and Engineering, Tsinghua University, Beijing 100084, P.R. China

<sup>b</sup>School of Advanced Materials, Shenzhen Graduate School, Peking University, Shenzhen 518055, P.R. China

<sup>c</sup>Key Laboratory for Radioactive Geology and Exploration Technology, Fundamental Science for National Defense, East China University of Technology, Nanchang, 330013, P.R. China.

<sup>#</sup> These authors contributed equally to this work

\*Corresponding Authors: Tel.: +86 10 62773741; fax: +86 10 62771100.

E-mail addresses: linyh@mail.tsinghua.edu.cn (Y.H. Lin)

Tel.: + 86 755 26033200;

E-mail addresses: panfeng@pkusz.edu.cn (F.P.)

## ABSTRACT:

We demonstrate that the confinement effect of the NiO compound can directly enhance the electrochemical performance upon cycling. Fabricating the core-shell C-coated Ni/NiO nanofibers (e.g., Ni and NiO, nitrogen doped carbon respectively) composite electrode largely increases the capacity ( $1332 \text{ mAh g}^{-1}$  vs  $718 \text{ mA h g}^{-1}$ ) and improve the long-term cycling stability. The High Angle Annular Dark Field results reveal that the doped pyridine-like nitrogen shell will divide the NiO into smaller nanoparticle during the charging and discharging process. In addition, the density functional theory calculation suggests the confined nanoscale NiO(Ni) will absorb and react with Li ions more easily. With cycling, smaller NiO/Ni nanoparticle will bring more active sites, leading additional interfacial lithiation capacity. At the same time, the confinement effect of the NiO compound further increases the capacity of the nanocomposites.

**Keywords:** confinement effect, lithium ion battery, core-shell nanostructure

## 1. Introduction

Li ion battery has been intensively utilized in portable electronics and show significant promise for applications [1-3]. The energy density and cycling performance of lithium ion batteries depend on the physical and chemical properties of both cathode and anode materials. Transitional metal oxides, such as NiO based nanomaterials have attracted considerable attention

as potential substitutes for graphite because of their numerous appealing features, including abundance, low cost, environmental benignity, and high theoretical capacity [4-7]. Nanostructured coating can restrain the volumetric change in the electrode and prevent the aggregation of the active materials which can enhance the cycling stability of batteries [8-12]. For lithium ion anode materials, an effective implementation of this concept is to use a multilayer thin film structure comprised of Si (or other high capacity materials) and inert metal layers (e.g., Ti, Al, and Zn) [10, 13-15]. Studies of Si-based multilayer electrodes show strong differences in reversible capacity and cycling stability as a function of the thicknesses of the buffer and active layers. The technical challenges of Li-alloying reactions (e.g., with Si) are similar to those found in the conversion reactions of metal oxides electrodes [10, 15]. As for the NiO, study results [16] show that the lithiation of NiO involve the formation and decomposition of  $\text{Li}_2\text{O}$ , with the reduction and oxidation of metal nano-particles in the range of 5–10 nm in diameter. In particular, nanoscale confinement of nanosized metal oxide particles is believed to improve the lithiation and delithiation electrochemical performance.

In order to explore the critical role of nanoscale confinement effect in electrochemical process of the formation/decomposition of  $\text{Li}_2\text{O}$ , we design a core-shell C-coated Ni/NiO nanofibers composite electrode. In particular, NiO is a promising anode material for LIBs due to its high theoretical specific capacity ( $718 \text{ mA h g}^{-1}$ ), abundant material supply and low cost. As NiO has low electronic conductivity, it is always composited with conductive materials. These composite anodes exhibited high reversible capacity and excellent electrochemical performance. However, the capacity of NiO based anode usually shows a decrease during lithiation and delithiation process due to the formation of the SEI layer [16-22]. Interestingly, the increase in cycling induced capacity has been found in the NiO and other metal oxide electrodes upon long cycles.

These phenomena may partly attribute to the activation of the conductive materials. Its origin arouses much attention and much effort has been devoted to the search. Nevertheless, the reason for the increased capacity with the cycling still remains unclear. One of the possible reasons is the lack of an effective model which can explain the activation mechanism based on experiment and calculation results. On the other hand, NiO based anodes are usually composited with other additives, increasing the difficulty to identify the confinement effect in electrochemical process.

Here, we design a core-shell C-coated Ni/NiO nanofibers composite electrode by employing the electrospinning and Chemical Vapor Deposition (CVD) methods. With the N-doped carbon coating, the core-shell C-coated Ni/NiO nanofibers exhibits remarkable reversible capacity and capacity retention. The formed nano reactor between the inner cavity of C-coated layer and NiO excludes other factor caused by the outside additives, and give an isolated space to explore the activation mechanism. The results find the nano reactor can facilitate effective lithiation and delithiation processes as well as NiO/Ni redox by confinement effect. In addition, the density functional theory calculation suggests that the confined NiO(Ni) can absorb and react with Li ions more easily.

## 2. Experimental

### 2.1. Synthesis of C-coated Ni/NiO nanofibers

Firstly, C-coated Ni/NiO nanofibers electrocatalysts were fabricated by electrospinning-chemical vapor deposition method. In detail, 0.8 g PVP and 0.45 g Ni(AC)<sub>2</sub>·4H<sub>2</sub>O were dissolved in 10 mL ethanol and then magnetically stirred at room temperature for 12 h.

Afterwards, the resulting homogeneous mixture was loaded into a spinneret which was linked to a high-voltage equipment with 15 KV working voltage. Aluminum foil was used as collector to gain the spinning sample at the rate of  $2 \text{ ml h}^{-1}$  by syringe pump in the relative humidity of 30%, and the primary spinning sample was heated at  $660 \text{ }^\circ\text{C}$  for 2 h at rate of  $2 \text{ }^\circ\text{C/min}$  in a furnace. After the heating treatment, sample was grinded and then placed on horizontal quartz tube of furnace. The furnace reaction chamber was evacuated and flushed with  $\text{N}_2$  for several times to remove oxygen and moisture, then the reactor was heated to  $800 \text{ }^\circ\text{C}$  at a rate of  $10 \text{ }^\circ\text{C/min}$  in  $\text{N}_2$ . 10 mL pyridine as precursor was injected into the reaction chamber for about 30 min by  $\text{N}_2$ . After the CVD reaction, a dark sponge-like product was obtained and labeled as C-coated Ni/NiO nanofibers .

## 2.2. Characterization

The morphology was observed with using field emission scanning electron microscopy (FE-SEM; JEOL JSM-7001F) and high-resolution transmission electron microscopy (HRTEM, JEOL2011). The chemical component was investigated by X-ray diffraction (XRD, Rigaku D/max-2500 instrument using  $\text{Cu K}\alpha$  radiation (40 kV) with a scanning rate of  $0.067 \text{ }^\circ/\text{s}$ ). The chemical state was performed with X-ray photoelectron spectroscopy (XPS, ultra-high-vacuum ESCALAB 250Xi electron spectrometer). The binding energies of XPS spectra refer to C 1s at 284.6 eV. Raman spectra were conducted on an INVIA spectrophotometer (Renishaw, UK).

## 2.3. Electrochemical test

CR2032 coin type half cells were fabricated in an argon-filled glovebox with Li metal as the counter electrode. 1M  $\text{LiPF}_6$  in ethyl carbonate/dimethyl carbonate (1:1 by volume) was used as electrolyte, and a porous polypropylene film (Celgard 2400, Celgard Inc., USA) was used to

separate the two electrodes. Charge/discharge tests were conducted at different current densities in a potential range of 0.01~3V vs. Li/Li<sup>+</sup> with a battery test system (C2001A, LAND, China). Cyclic voltammograms (CV) measurements were carried out at a scan rate of 0.1 mV s<sup>-1</sup> between 0.01 and 3 V using CHI760 Battery Tester.

#### 2.4. Calculation Method

The DFT calculations were performed by using the Vienna Ab-initio Simulation Package (VASP) [23] using local-density approximation (LDA) exchange-correlation functional with Projector augmented-wave method (PAW) [24-26]. The cut-off energy is set to be 450 eV and a k-points mesh is set to be 6×6×1 including gamma point. During the geometry optimizations, the lattice constants were fixed. A vacuum buffer space of 20 Å is set above lithium atoms. The lithium atom adsorption was calculated on a six-layer 2×2 nickel (111) slab. For each ratio, we calculated two or three possible arrangement of lithium atom on the surface.

## 3. Results and discussion

### 3.1 Structure and morphology of the C-coated Ni/NiO nanofibers nanofibers

The XRD patterns of NiO nanofibers and C-coated Ni/NiO nanofibers are shown in Fig. 1a. It is seen that peaks for the two samples at  $\theta = 37.2^\circ, 43.4^\circ, 62.9^\circ, 75.2^\circ$  and  $79.4^\circ$  should be assigned well to (111), (200), (220), (311) and (222) diffraction of NiO (JCPDS 65-6920). After CVD treatment, new diffraction peaks for C-coated Ni/NiO nanofibers can be seen at  $44.2^\circ, 51.6^\circ$ , and  $76.1^\circ$  corresponding to (111), (200), and (220) of Ni (JCPDS 65-0380), respectively. Moreover, the intensity of NiO diffraction peaks was reduced over C-coated Ni/NiO nanofibers

due to the existence of Ni, indicating partial NiO was reduced into Ni in the process of carbon coating by the CVD treatment. The XRD diffraction peaks for carbon layers can be probed at  $21.2^\circ$ ,  $30.3^\circ$ ,  $31.6^\circ$ ,  $76.1^\circ$ , which may be attributed to the produced C-coated layer. Raman spectroscopy is often used to investigate the production and its graphitization structure of carbon nano materials. As seen in Fig. 1b C-coated Ni/NiO nanofibers sample presents two primary peaks at  $1342$  and  $1576\text{ cm}^{-1}$  corresponding to the vibrations of carbon atoms in the disordered graphite structure (i.e., defects, named D band) and the  $E_{2g}$  mode of graphite (i.e., graphite structure, named G band), and thus the intensity ratio of G band to D band ( $I_G/I_D$ ) presents the graphitization degree. In Fig. 1b, we can see that  $I_G/I_D$  is about 0.6, indicating the existence of poor graphite structure for C-coated Ni/NiO nanofibers .

To further investigate the surface composition of NiO nanofiber and C-coated Ni/NiO nanofibers , the XPS spectra (Fig. 1c) of Ni 2p for the two samples distributes the regions of 850-857.5 eV and 857.5-866 eV, corresponding to Ni 2p<sub>3/2</sub> and satellite peak. The Ni 2p<sub>3/2</sub> peak of two samples can be deconvoluted into two components centered at 871.8 and 874.89 eV, ascribable to the characteristic of Ni<sup>2+</sup> and Ni species, respectively. A quantitative analysis based on the integrated area of two decomposed peaks could give rise to the relative proportion of Ni to Ni<sup>2+</sup> species. The molar ratio of Ni/Ni<sup>2+</sup> is 1.6:1 and 1:2.4 for NiO nanofiber and C-coated Ni/NiO nanofibers , suggesting the existence of Ni after coating.

Fig. 2a presents the morphologies and structures of the samples examined by TEM. We can see that NiO nanofiber was coated with carbon. Moreover, NiO nanofiber with length of 600-800 nm were continuous dispersed in the C-coated layer, thus the formed nano reactor between the inner cavity of C-coated layer and NiO is beneficial to lithiation and delithiation processes as well as NiO/Ni redox by confinement effect. In Fig. 2b, the lattice fringes with a spacing of 0.24



nm were observed in the C-coated Ni/NiO nanofibers, corresponding to the (111) plane of NiO. The ring-like mode in the selected-area electron diffraction (SAED) pattern can confirm the NiO species in the C-coated Ni/NiO nanofibers.

### 3.2 Electrochemical performance

The electrochemical activity of the prepared anode electrodes was firstly tested at a  $200 \text{ mA g}^{-1}$  in Fig. 3a. NiO nanofiber electrode can only achieve an initial charge capacity of  $743 \text{ mAh g}^{-1}$ , and the charge capacity continuously decreases with cycling, and drop to  $383 \text{ mAh g}^{-1}$  after 40<sup>th</sup> cycle because of the growth of SEI film, with the charge capacity efficiency reduced by 52%. Nevertheless, initial charge capacity of C-coated Ni/NiO nanofibers electrode can reach at  $545 \text{ mAh g}^{-1}$ , moreover, the charge capacity efficiency continuously increases by 22.4%, and reached  $667 \text{ mAh g}^{-1}$  after 40<sup>th</sup> cycle. Combined with Fig. 1 and 2, we can see the electrocatalytic activity of C-coated Ni/NiO nanofibers was enhanced by the improved composites, morphology, and electronic characteristics by coating with carbon layer. In Fig. 3b, the reversible capacities of C-coated Ni/NiO nanofibers can reach to  $1662 \text{ mAh g}^{-1}$  at a current density of  $0.1 \text{ A g}^{-1}$ . As the current densities varied from  $0.1$  to  $2 \text{ A g}^{-1}$ , the specific capacity can be recovered to  $1332 \text{ mAh g}^{-1}$ , which C-coated Ni/NiO nanofibers presents good charge-discharge capability. Fig. 3c shows the potential versus capacity profiles of C-coated Ni/NiO nanofibers during the 1st, 2nd, and 3rd cycles at  $100 \text{ mA g}^{-1}$ . The charging/discharging profiles of C-coated Ni/NiO nanofibers are similar in the cycles process. The first discharging capacity of C-coated Ni/NiO nanofibers is  $1600 \text{ mAh g}^{-1}$ , which is much higher than the previous reported electrocatalysts. Moreover, the potentials of C-coated Ni/NiO nanofibers at approximately  $1.0 \text{ V}$  in these cycles, indicate the highly efficient conversion between NiO and Ni ( $\text{NiO} + 2\text{Li} \rightleftharpoons \text{Li}_2\text{O} + \text{Ni}$ ) due to the confinement effect of C-coated layer.

To verify the assumption, Ni/NiO was fabricated according to pulsed laser deposition and used as the cathode in the charge and discharge test of lithium battery. The recycle electrocatalytic performances of Ni/NiO and C-coated Ni/NiO nanofibers were shown in Fig. 3d at 200mA rate. The first discharge capacity over Ni/NiO reached to 1092 mAh g<sup>-1</sup>, however, the capacity for Ni/NiO decreased to 907 mAh g<sup>-1</sup> in the second recycle. More positively, compared with Ni/NiO electrocatalyst, C-coated Ni/NiO nanofibers shows a higher reversible electrocapacity and retention. In Fig. 3d, it can be seen that the electrocatalytic capacity over C-coated Ni/NiO nanofibers increased to 1046 mAh g<sup>-1</sup> after 100 cycles. Therefore, C-coated Ni/NiO nanofibers presents high electrocatalytic activity and stability due to the confinement effect of C-coated layer on the redox of NiO/Ni as well as the adsorption and insertion of lithium ion in the charge and discharge process of lithium battery.

In order to confirm effective redox capability between NiO to Ni with the aid of C-coated layer confinement effect, the morphology and composition of C-coated Ni/NiO nanofibers were investigated after charge-discharge recycle. The HAADF result shows that, compared with the size before lithiation, Ni/NiO NPs were smaller with the size of 5-180 nm, as illustrated in Fig. 4a, and the corresponding TEM and HRTEM show that Ni/NiO species diffused into nano layer of C-coated layer, as confirmed by EDS characterization[27]. Moreover, we investigated the adsorption behavior of Li<sup>+</sup> on Ni (111) crystal surface by calculating binding energy between Li atoms and nickel clusters. In Fig. 5, it is seen that the binding energy is -1.37eV when the ratio of Li<sup>+</sup>/Ni is 0.25, indicating Li ions were preferentially adsorbed on the surface of Ni. Furthermore, the binding energy remain negative when increasing the ratio of Li<sup>+</sup>/Ni from 0.25 to 2.5. When the ratio of Li<sup>+</sup>/Ni increased to 2.75, the binding energy shows the positive value, suggesting the accumulated Li ions enhance the adsorption energy barrier. The calculation results show that the

nano scale Ni/NiO can store 25 percent Li more than theoretical value. On the other hand, the result indicates the reaction of  $\text{Li}_2\text{O}$  to  $\text{Li}_2\text{O}_2$ . Usually, the reaction of  $\text{Li}_2\text{O}$  to  $\text{Li}_2\text{O}_2$  does not happen because the highly insulating  $\text{Li}_2\text{O}_2$  can automatically shut down the reaction [28]. However the smaller NiO particle upon the cycling may acts as catalyst in such a reaction. Therefore, the smaller NiO particles provide more active surface area and may act as catalyst in the reaction of  $\text{Li}_2\text{O}$  to  $\text{Li}_2\text{O}_2$ .

## 4. Conclusions

In summary, the C-coated Ni/NiO nanofibers were prepared by a simple electrospinning approach followed by CVD reaction. The specific combination of composition shows superior features with a specific discharge capacity of  $1662 \text{ mA g}^{-1}$  at a current density of  $0.1 \text{ A g}^{-1}$ . Experimental evidence confirm the N-doping brings multifold revolutionary effects on the Li storage of Ni/NiO hybrid composite electrodes. The increasing active sites of NiO serves as a major contributor to the enhanced capacity upon long cycling. The confinement effect of the nano scale NiO effectively enhancing the electrochemical performance and showed a better characteristic in storing lithium. Our finding will shed new light on understanding of oxide conversion reactions in lithium ion batteries, guiding new nanostructure design of N-coating metal-oxide-based electrodes. The possibility of nanoscale NiO promoting the reversible formation and decomposition of  $\text{Li}_2\text{O}_2$  may inspire the study of the Li- $\text{O}_2$  cells.

## Conflict of interest

The authors declare that they have no conflict of interest

## Acknowledgment

This work was supported by the NSF of China (Grant No. 51532002).

## References

- 1 Thomas J. Lithium batteries: A spectacularly reactive cathode. *Nature Mater.* 2 (2003) 705-706.
- 2 Kang K, Meng YS, Bréger J, et al. Electrodes with high power and high capacity for rechargeable lithium batteries. *Science* 311 (2006) 977-980.
- 3 Armand M, Tarascon JM. Building better batteries. *Nature* 451 (2008) 652-657.
- 4 Kang N, Park JH, Choi J, et al. Nanoparticulate iron oxide tubes from microporous organic nanotubes as stable anode materials for lithium ion batteries. *Angew. Chem. Int. Ed.* 51 (2012) 6626-6630.

- 5 Guo J, Liu Q, Wang C, et al. Interdispersed Amorphous MnO<sub>x</sub>-Carbon Nanocomposites with Superior Electrochemical Performance as Lithium-Storage Material. *Adv. Funct. Mater.* 22 (2012) 803-811.
- 6 Dirican M, Lu Y, Ge Y, et al. Carbon-confined SnO<sub>2</sub>-electrodeposited porous carbon nanofiber composite as high-capacity sodium-ion battery anode material. *ACS Appl. Mater. Interfaces* 7 (2015) 18387.
- 7 Huang H, Feng T, Gan Y, et al. TiC/NiO core/shell nanoarchitecture with battery-capacitive synchronous lithium storage for high-performance lithium-ion battery. *ACS Appl. Mater. Interfaces* 7 (2015) 11842.
- 8 Xu B, Luo Y, Liu T, et al. Ultrathin N-doped carbon-coated TiO<sub>2</sub> coaxial nanofibers as anodes for lithium ion batteries. *Jam Ceram Soc.* (2017) 1-9.
- 9 Tan G, Wu F, Yuan Y, et al. Freestanding three-dimensional core-shell nanoarrays for lithium-ion battery anodes. *Nature Commun.* 7 (2016) 11774.
- 10 Wang C, Wu H, Chen Z, et al. Self-healing chemistry enables the stable operation of silicon microparticle anodes for high-energy lithium-ion batteries. *Nature Chem.* 5 (2013) 1042-1048.
- 11 Raccichini R, Varzi A, Chakravadhanula VS, et al. Boosting the power performance of multilayer graphene as lithium-ion battery anode viaunconventional doping with in-situ formed fe nanoparticles. *Sci. Rep.* 6 (2016) 23585.
- 12 Fu K, Yildiz O, Bhanushali H, et al. Aligned carbon nanotube-silicon sheets: A novel nano-architecture for flexible lithium ion battery electrodes. *Adv. Mater.* 25 (2013) 5109-5114.

- 13 Zhang WJ. A review of the electrochemical performance of alloy anodes for lithium-ion batteries. *J. Power Sources*. 196 (2011) 13-24.
- 14 Wang G X, Sun L, Bradhurst D H, et al. Nanocrystalline NiSi alloy as an anode material for lithium-ion batteries. *Journal of Alloys and Compounds* 306 (2000) 249-252.
- 15 McDowell MT, Lee SW, Harris JT, et al. In situ TEM of two-phase lithiation of amorphous silicon nanospheres. *Nano Lett.* 13 (2013) 758-764.
- 16 Wu H, Chan G, Choi JW, et al. Stable cycling of double-walled silicon nanotube battery anodes through solid-electrolyte interphase control. *Nature Nanotech.* 7 (2012) 310-315.
- 17 Wu H, Zheng G, Liu N, et al. Engineering empty space between Si nanoparticles for lithium-ion battery anodes. *Nano Lett.* 12 (2012) 904-909.
- 18 Zhou X, Wan LJ, Guo YG. Binding SnO<sub>2</sub> Nanocrystals in Nitrogen-Doped Graphene Sheets as Anode Materials for Lithium-Ion Batteries. *Adv. Mater.* 25 (2013) 2152-2157.
- 19 Gu Y, Wu F, Wang Y. Confined volume change in Sn-Co-C ternary tube-in-tube composites for high-capacity and long-life lithium storage. *Adv. Funct. Mater.* 23 (2013) 893-899.
- 20 Zhang J, Yu A. Nanostructured transition metal oxides as advanced anodes for lithium-ion batteries. *Science bulletin*, 60 (2015) 823-838.
- 21 Wu H, Chan G, Choi JW, et al. Stable cycling of double-walled silicon nanotube battery anodes through solid-electrolyte interphase control. *Nature Nanotech.* 7 (2012) 310-315.
- 22 Evmenenko G, Fister T T, Buchholz D B, et al. Morphological evolution of multilayer Ni/NiO thin film electrodes during lithiation. *ACS Appl. Mater. Interfaces* 8 (2016) 19979-19986.
- 23 Kresse G, Furthmüller J. Efficient iterative schemes for ab initio total-energy calculations

- using a plane-wave basis set. *Phys Rev B* 54(16) (1996) 11169.
- 24 Kohn W, Sham L J. Self-consistent equations including exchange and correlation effects. *Phys. Rev.* 140(4A) (1965) A1133.
- 25 Blöchl P E. Projector augmented-wave method. *Phys. Rev. B* 50(24) (1994) 17953.
- 26 Kresse G, Joubert D. From ultrasoft pseudopotentials to the projector augmented-wave method. *Phys. Rev. B* 59(3) (1999) 1758.
- 27 Shin WH, Jeong HM, Kim BG, et al. Nitrogen-doped multiwall carbon nanotubes for lithium storage with extremely high capacity. *Nano lett.* 12 (2012) 2283-2288.
- 28 Huang Y, Xu Z, Mai J, et al. Revisiting the origin of cycling enhanced capacity of Fe<sub>3</sub>O<sub>4</sub> based nanostructured electrode for lithium ion batteries. *Nano Energy* 2017.

## Figure caption

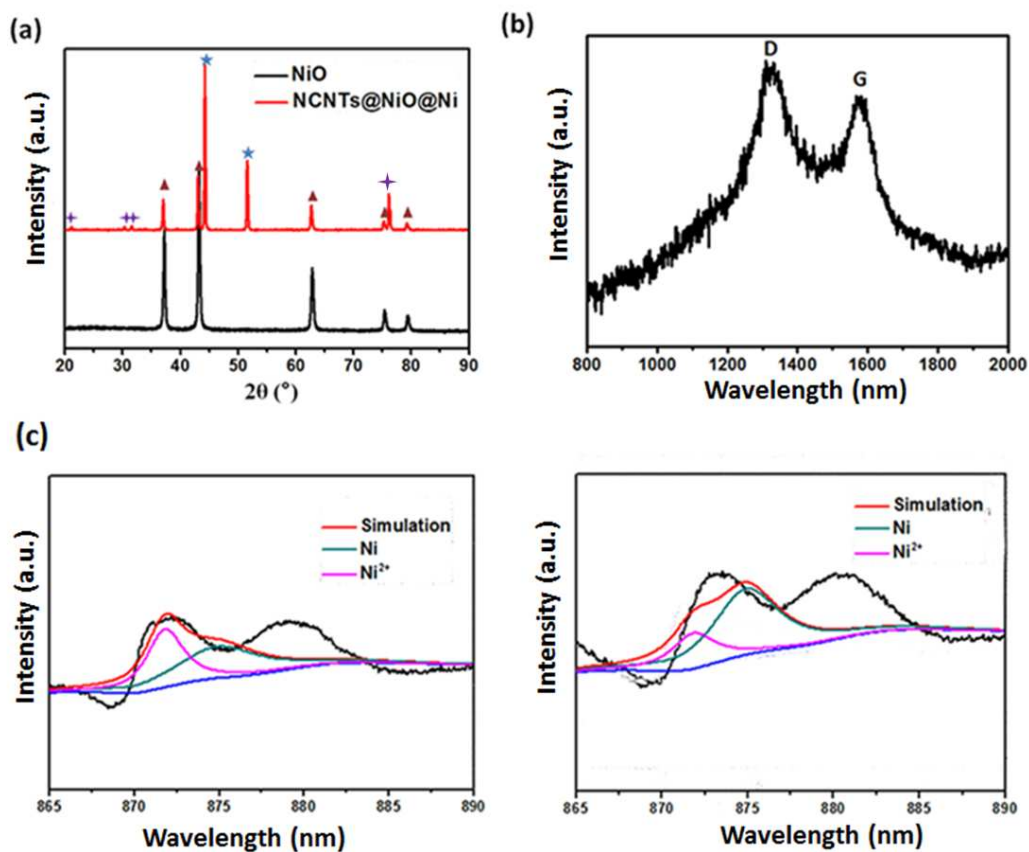


**Figure 1** (a) XRD patterns and (b) Raman spectra of C-coated Ni/NiO nanofibers array; (c) XPS spectra of NiO@Ni before and after coating (left and right).

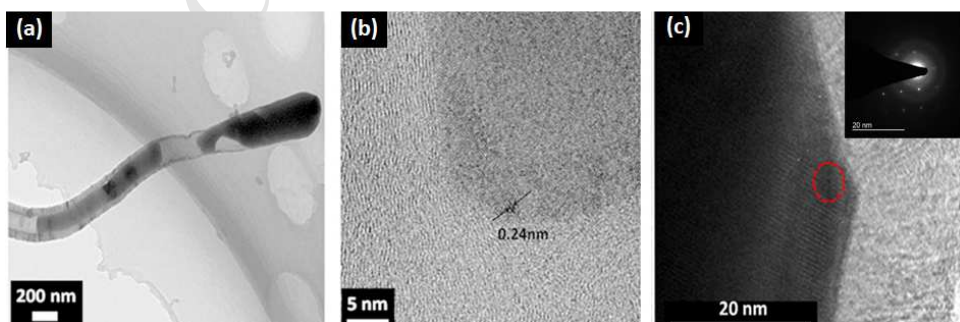




**Figure 2** (a) A TEM image of C-coated Ni/NiO nanofibers ; (b),(c) HRTEM image of C-coated Ni/NiO nanofibers ; Inset: SAED of C-coated Ni/NiO nanofibers .

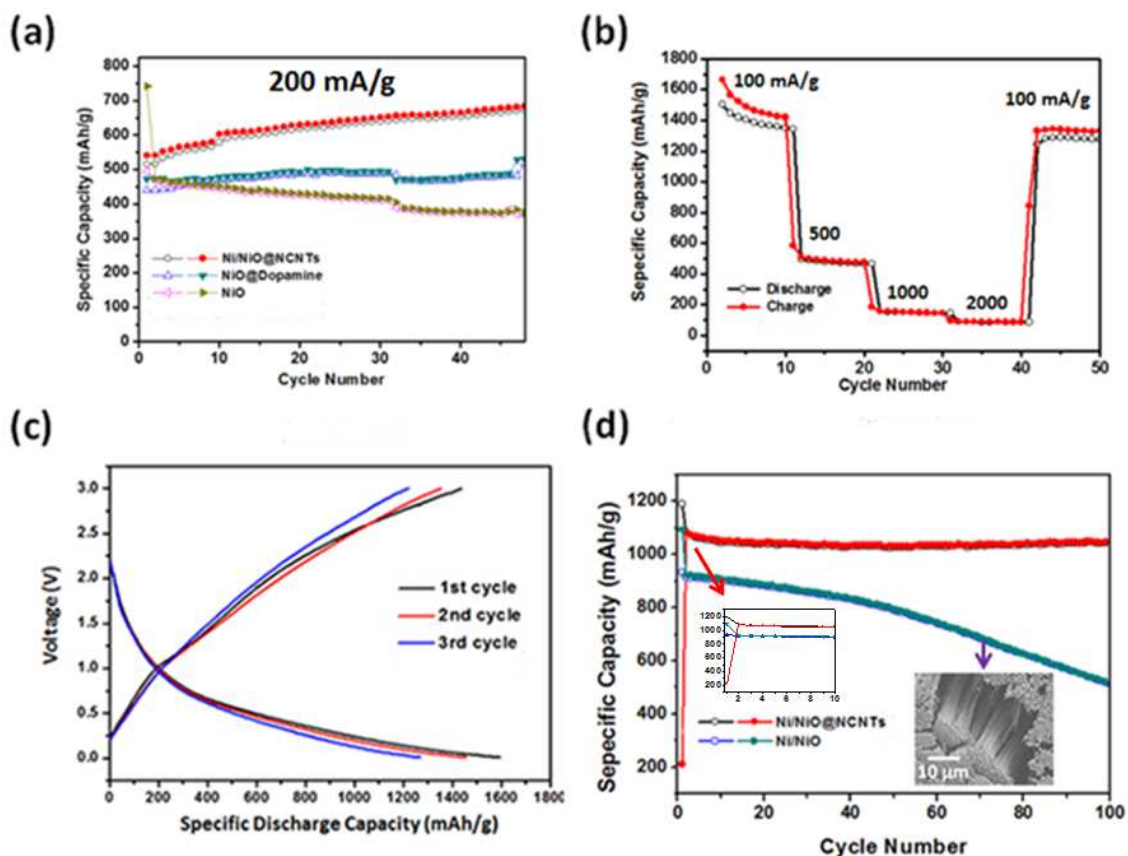


**Figure 3** (a) Cycling performance at 200 mA g<sup>-1</sup> of C-coated Ni/NiO nanofibers , NiO@Dopamine, NiO; (b) Rate performance of C-coated Ni/NiO nanofibers at different current densities from 0.1 to 2 A g<sup>-1</sup> (Hollow: discharge; solid: charge); (c) Charge-discharge curves of C-coated Ni/NiO nanofibers at 100 mA g<sup>-1</sup>; (d) Cycling performance at 200 mA g<sup>-1</sup> of C-coated Ni/NiO nanofibers array. Inset: SEM images of the Ni@NiO arrays.

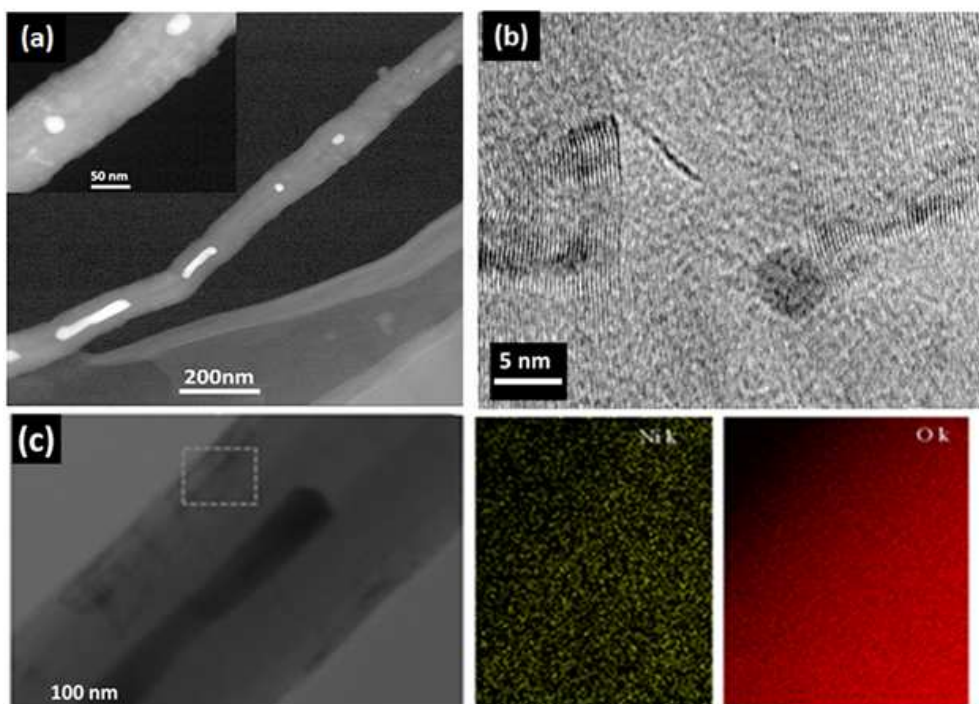


**Figure 4** (a) HAADF images of the C-coated Ni/NiO nanofibers after the lithiation; (b) TEM images of the C-coated Ni/NiO nanofibers after the lithiation; (c) TEM image and the EDS elemental mapping of the C-coated layer@NiO@Ni.

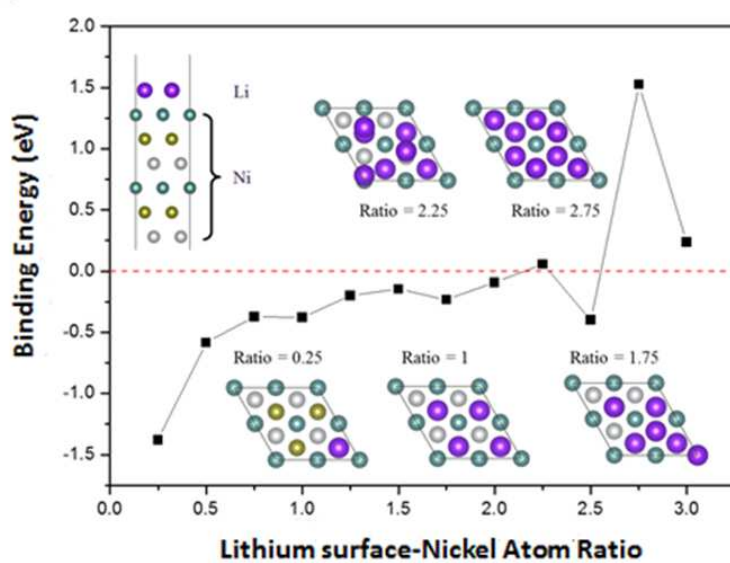


**Figure 5** Binding energy with different lithium surface-nickel atom ratios. The inset figures indicate configurations of different lithium atom numbers. Different nickel atoms are in different colors according to their positions.

ACCEPTED MANUSCRIPT

- The core–shell Carbon-coated Ni/NiO exhibits the remarkable reversible capacity and capacity retention.
- The confinement effect of coating layer brings multifold revolutionary effects on the Li storage.
- The density functional theory calculation suggests the confined nanoscale NiO(Ni) will be easier to absorb and react with Li ions